

Bifurcation Structure in the Hydrogen Peroxide–Sulfite System

Ichiro Hanazaki,* Nobuko Ishibashi, Hiroko Mori, and Yoshifumi Tanimoto

Department of Chemistry, Faculty of Science, Hiroshima University, 1-3-1 Kagamiyama, Higashi-Hiroshima 739-8526, Japan

Received: March 30, 2000

Bifurcation structure of the hydrogen peroxide–sulfite system was examined quantitatively under the flow condition, from which rate constants k_2 and k_3 and equilibrium constant K_1 for the skeleton reactions $\text{H}^+ + \text{SO}_3^{2-} \leftrightarrow \text{HSO}_3^-$ (1); $\text{HSO}_3^- + \text{H}_2\text{O}_2 \rightarrow \text{H}^+ + \text{SO}_4^{2-} + \text{H}_2\text{O}$ (2); and $\text{H}^+ + \text{HSO}_3^- + \text{H}_2\text{O}_2 \rightarrow 2\text{H}^+ + \text{SO}_4^{2-} + \text{H}_2\text{O}$ (3) were determined at 13.2, 20.0, 25.0, and 32.0 °C. The results are summarized as k_2 ($\text{M}^{-1}\text{s}^{-1}$) = $(1.19 \times 10^6)\exp(-\Delta H_2^\ddagger/\text{RT})$, $\Delta H_2^\ddagger = 28.2 \text{ kJ}\cdot\text{M}^{-1}$; k_3 ($\text{M}^{-2}\text{s}^{-1}$) = $(5.93 \times 10^9)\exp(-\Delta H_3^\ddagger/\text{RT})$, $\Delta H_3^\ddagger = 18.7 \text{ kJ}\cdot\text{M}^{-1}$; K_1 (M^{-1}) = $(1.8 \times 10^6)\exp(-\Delta H_1/\text{RT})$, $\Delta H_1 = 7.4 \text{ kJ}\cdot\text{M}^{-1}$. The system is well known to exhibit chemical oscillations in its pH value when it is combined with an appropriate species that provides a negative feedback channel. However, the role of the nonlinearity inherent in this subsystem has not been clarified sufficiently under the flow condition. In the present work, we proposed an approximate analytical method to analyze the complicated equations representing the bifurcation structure and succeeded in determining the above constants and their temperature dependence. The present results are expected to be useful in designing a new chemical oscillator system by coupling this subsystem with appropriate negative-feedback species. In addition, the information given here for the temperature dependence would be useful to design the temperature-insensitive chemical oscillator system which is interested recently in relation to the function in living systems.

1. Introduction

The hydrogen peroxide–sulfite system is known to exhibit nonlinear behaviors such as bistability in the acidic aqueous solution and chemical oscillations in pH when it is coupled with ferrocyanide under the flow condition.^{1,2} However, it has been known that the $\text{H}_2\text{O}_2\text{–Fe}(\text{CN})_6^{4-}\text{–H}^+$ system, which does not contain SO_3^{2-} as a reductant, does show oscillations.^{3–5} It has been shown that a special reaction scheme based on the unstable intermediates produced from $\text{Fe}(\text{CN})_6^{4-}$ is responsible for the oscillations.^{3–5} A study of visible light pulse illumination on the $\text{H}_2\text{O}_2\text{–Fe}(\text{CN})_6^{4-}\text{–H}^+$ system has also supported the importance of reactions related to ferrocyanide.⁴ In other words, the nonlinearity inherent in the $\text{H}_2\text{O}_2\text{–SO}_3^{2-}\text{–H}^+$ tends to be concealed by the nonlinearity peculiar to $\text{Fe}(\text{CN})_6^{4-}$.

The combination of the $\text{H}_2\text{O}_2\text{–SO}_3^{2-}\text{–H}^+$ subsystem with marble has been shown to exhibit chaotic oscillations.⁶ This work is important, for it has first shown that the substance other than ferrocyanide (in this case CO_3^{2-} or HCO_3^- from solid marble) can produce chemical oscillations, or even more complex behavior such as chemical chaos. However, for the purpose of establishing a general nonlinear behavior in the $\text{H}_2\text{O}_2\text{–SO}_3^{2-}\text{–H}^+$ subsystem, the existence of solid–liquid interface in the marble system makes the analysis of the reaction mechanism more or less complex. Later, the homogeneous solution system with the carbonate ion was shown to exhibit chemical oscillations.⁷ The system with ferrocyanide and HCO_3^- has also been shown to exhibit chaotic oscillations.⁸ A light-induced chaos has also been reported for the same system.⁹ However, even for these systems we encounter a difficulty since there is a possibility of escaping of carbonate as CO_2 during the oscillations, which naturally incorporates the liquid–gas interphase problem. It is desirable to find an easier-to-handle partner to be combined with the subsystem.

In the analogous pH oscillator, $\text{BrO}_3^- \text{–SO}_3^{2-} \text{–Fe}(\text{CN})_6^{4-} \text{–H}^+$, the role of the intrinsic nonlinearity in the $\text{BrO}_3^- \text{–SO}_3^{2-} \text{–H}^+$

subsystem is much clearer.^{10–14} In addition, for the latter system, Mn^{2+} or MnO_2^- , used in place of $\text{Fe}(\text{CN})_6^{4-}$, has recently been found to exhibit chemical oscillations, suggesting many other metal ions or metal complexes could be coupled to give new chemical oscillator systems.¹⁵

Some rate constants inherent to the system with $\text{H}_2\text{O}_2/\text{SO}_3^{2-}$ are given in the literature.^{16,17} Unfortunately, they were measured at one or two temperatures, which are insufficient for discussing the temperature effect. Moreover, they were measured in a batch system or with the stopped flow technique, not in the continuous flow system. Recently, studies on nonlinear behaviors of such systems have been done mostly under the flow condition, and it is desirable to determine the bifurcation structure of the subsystem as well as the rate constant values directly under the CSTR (continuous-flow stirred tank reactor) condition.

We have recently found a temperature-compensation effect in the $\text{H}_2\text{O}_2\text{–S}_2\text{O}_3^{2-}\text{–SO}_3^{2-}$ pH-oscillator system, for which the period of chemical oscillations is almost unchanged between 25.5 and 33.5 °C.¹⁸ We believe that this result is of importance in relation to the mechanism of biological clocks, and that more accurate determination of the temperature dependence of the rates of key reaction steps in the fundamental subsystem, $\text{H}_2\text{O}_2\text{–SO}_3^{2-}\text{–H}^+$, is required.

In view of this situation, we have tried to determine the nonlinear reaction mechanism in the $\text{H}_2\text{O}_2\text{–SO}_3^{2-}\text{–H}^+$ subsystem directly and quantitatively by establishing its bifurcation structure in the temperature range of 13–32 °C. The results would be helpful in understanding the fundamental system characteristics and also in obtaining a basis to expand a possibility of finding new partners with which the subsystem could give rise to chemical oscillations and other nonlinear behaviors.

2. Experimental Section

Commercially available reagents, H_2O_2 (GR, ca. 31%; Mitsubishi Gas Chemicals), Na_2SO_3 (GR; Kanto Chemicals), H_2O

* To whom correspondence should be addressed: (e-mail) hanazaki@sci.hiroshima-u.ac.jp; (fax) +81-(0)824-24-0731.

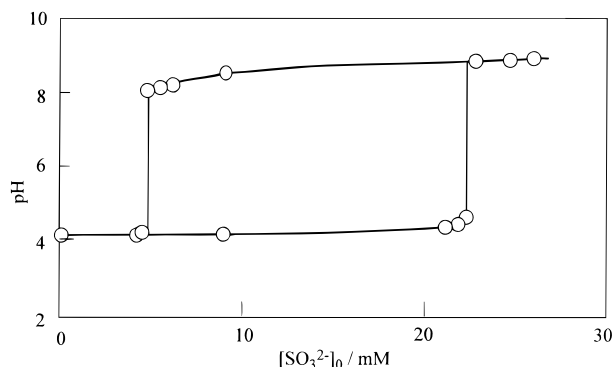


Figure 1. Bifurcation diagram at 32.0 °C. $[\text{H}_2\text{O}_2]_0 = 29.8 \text{ mM}$, $[\text{H}^+]_0 = 1.15 \times 10^{-4} \text{ M}$ and $k_0 = 8.70 \times 10^{-3} \text{ s}^{-1}$.

SO_4 (> 97%; Katayama Chemicals), were used as received. All measurements were performed under the CSTR condition. The stock solution of H_2O_2 was freshly prepared for each run, the concentration of which is determined by the iodometry. Three stock solutions were introduced into a flow cell by a peristaltic pump (Eyela MP-3) at a constant flow rate and stirred rigorously by a magnetic stirrer (Iuchi, M3 + MS101). The volume of the reaction mixture in the cell was kept at $V = 10.4 \text{ mL}$ by pumping it with an aspirator (Yamato, mp-15). The rate of flow is conveniently characterized by $k_0 [\text{s}^{-1}] \equiv v/V$, where $v [\text{mLs}^{-1}]$ is the total flow rate. The initial concentration ($[\text{H}_2\text{O}_2]_0$, etc.) is defined for each species to be the concentration of the species in the cell calculated on the assumption that no reaction took place in the cell.

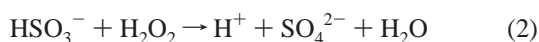
The cell was thermostated by circulating water, the temperature of which was maintained constant with a temperature controller (Eyela, ECS-0 + SB-9). The pH of the solution was measured by a pH electrode (Horiba, 6366) with a pH meter (Horiba D-13), and processed by a personal computer (NEC 9801-VX).

In the following, bifurcation structures are determined at four different temperatures, 13.2, 19.0, 25.0, and 32.0 °C. Among the experimental variables, $k_0 = 8.70 \times 10^{-3} \text{ s}^{-1}$ and $[\text{H}^+]_0 = 1.15 \times 10^{-4} \text{ M}$ are fixed throughout, while $[\text{H}_2\text{O}_2]_0$ and $[\text{SO}_3^{2-}]_0$ are treated as variable parameters.

3. Results and Analysis

3-1. General Considerations. Figure 1 illustrates the bistability of the system observed at 32.0 °C by changing $[\text{SO}_3^{2-}]_0$ with fixed $[\text{H}_2\text{O}_2]_0$ and k_0 . We have performed similar measurements for different $[\text{H}_2\text{O}_2]_0$ values to determine the critical $[\text{SO}_3^{2-}]_0$ values ($[\text{SO}_3^{2-}]_{0c}$) for the neutral-to-acidic and acidic-to-neutral bifurcations, respectively. Results are summarized in Table 1. A state diagram spanned by $[\text{H}_2\text{O}_2]_0$ and $[\text{SO}_3^{2-}]_0$ can be drawn on the basis of the results in Table 1 and is shown in Figure 2 for 32.0 °C.

Now for the purpose of analyzing the results to establish the nonlinearity in the system, the reaction scheme (1) – (3) below is employed following the previous work.^{1,2,6}



Corresponding rate equations are

$$\begin{aligned} d[\text{H}^+]/dt &= k_{-1}[\text{HSO}_3^-] - k_1[\text{H}^+][\text{SO}_3^{2-}] + k_2[\text{H}_2\text{O}_2] \\ &[\text{HSO}_3^-] + k_3[\text{H}_2\text{O}_2][\text{H}^+][\text{HSO}_3^-] + k_0([\text{H}^+]_0 - [\text{H}^+]) \end{aligned} \quad (4)$$

TABLE 1: Experimentally Determined Bifurcation Points^a

	neutral-to-acidic bifurcation		acidic-to-neutral bifurcation	
	$[\text{H}_2\text{O}_2]_0/\text{mM}$	$[\text{SO}_3^{2-}]_{0c}/\text{mM}$	$[\text{H}_2\text{O}_2]_0/\text{mM}$	$[\text{SO}_3^{2-}]_{0c}/\text{mM}$
(13.2 °C)	4.30	0.92		
	8.61	1.54	8.61	8.1
	12.9	1.93	12.9	11.1
	21.51	2.3	21.5	15.1
	30.1	2.6	30.1	19.1
	38.7	3.4	38.7	21.4
(20.0 °C)	8.41	1.92	8.42	7.6
	12.6	2.32	12.6	10.33
	16.8	2.4	16.8	12.9
	25.3	3.0	25.3	17.4
	33.7	3.9	33.7	20.1
	(25.0 °C)	4.25	1.25	
8.50		1.76	8.50	8.23
12.8		2.2	12.8	10.8
17.0		2.6	17.0	14.0
25.5		3.8	25.5	18.1
34.0		4.7	34.0	21.8
(32.0 °C)	4.25	1.29		
	8.50	1.86	8.50	7.96
	12.8	2.34	12.8	11.8
	17.0	3.7	17.0	13.6
	25.5	4.2	25.5	18.6
	34.0	5.5	34.0	23.6

^a For a given value of $[\text{H}_2\text{O}_2]_0$, the critical concentration, $[\text{SO}_3^{2-}]_{0c}$, of sulfite ion to cause bifurcations is shown.

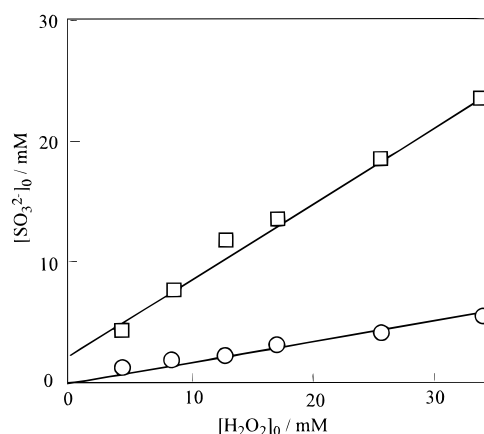


Figure 2. State diagram at 32.0 °C. $[\text{H}^+]_0 = 1.15 \times 10^{-4} \text{ M}$ and $k_0 = 8.70 \times 10^{-3} \text{ s}^{-1}$. Circles and squares represent the neutral-to-acidic and acidic-to-neutral bifurcation points, respectively.

$$\begin{aligned} d[\text{SO}_3^{2-}]/dt &= k_{-1}[\text{HSO}_3^-] - k_1[\text{H}^+][\text{SO}_3^{2-}] + \\ &k_0([\text{SO}_3^{2-}]_0 - [\text{SO}_3^{2-}]) \end{aligned} \quad (5)$$

$$\begin{aligned} d[\text{HSO}_3^-]/dt &= k_1[\text{H}^+][\text{SO}_3^{2-}] - k_{-1}[\text{HSO}_3^-] - k_2[\text{H}_2\text{O}_2] \\ &[\text{HSO}_3^-] - k_3[\text{H}_2\text{O}_2][\text{H}^+][\text{HSO}_3^-] - k_0[\text{HSO}_3^-] \end{aligned} \quad (6)$$

$$\begin{aligned} d[\text{H}_2\text{O}_2]/dt &= -k_2[\text{H}_2\text{O}_2][\text{HSO}_3^-] - \\ &k_3[\text{H}_2\text{O}_2][\text{H}^+][\text{HSO}_3^-] + k_0([\text{H}_2\text{O}_2]_0 - [\text{H}_2\text{O}_2]) \end{aligned} \quad (7)$$

Under the stationary condition, $d[\text{H}^+]/dt = d[\text{SO}_3^{2-}]/dt = d[\text{HSO}_3^-]/dt = d[\text{H}_2\text{O}_2]/dt = 0$, eqs 4, 6, 5, and 7 give

$$[\text{H}_2\text{O}_2] = -[\text{SO}_3^{2-}]_0 + [\text{SO}_3^{2-}] + [\text{H}_2\text{O}_2]_0 + [\text{H}^+]_0 - [\text{H}^+] \quad (8)$$

$$[\text{HSO}_3^-] = [\text{H}^+]_0 - [\text{H}^+] \quad (9)$$

$$k_1[\text{H}^+][\text{SO}_3^{2-}] = k_{-1}([\text{H}^+]_0 - [\text{H}^+]) + k_0([\text{SO}_3^{2-}]_0 - [\text{SO}_3^{2-}]) \quad (10)$$

$$\{(k_2 + k_3[\text{H}^+])([\text{H}^+]_0 - [\text{H}^+]) + k_0\}([\text{SO}_3^{2-}]_0 - [\text{SO}_3^{2-}] - [\text{H}^+]_0 + [\text{H}^+]) = (k_2 + k_3[\text{H}^+])([\text{H}^+]_0 - [\text{H}^+])[\text{H}_2\text{O}_2]_0 \quad (11)$$

Then eq 10 gives

$$[\text{SO}_3^{2-}] = \{k_{-1}([\text{H}^+]_0 - [\text{H}^+]) + k_0[\text{SO}_3^{2-}]_0\} / (k_1[\text{H}^+] + k_0) \quad (12)$$

Assuming k_1 and k_{-1} to be large, eq 12 becomes

$$[\text{SO}_3^{2-}] = ([\text{H}^+]_0 - [\text{H}^+]) / K_1[\text{H}^+] \quad (13)$$

where $K_1 \equiv k_1/k_{-1}$. Equations 11 and 13 then give

$$\{(k_2 + k_3[\text{H}^+])([\text{H}^+]_0 - [\text{H}^+]) + k_0\} \{K_1[\text{H}^+]([\text{SO}_3^{2-}]_0 - [\text{H}^+]_0 + [\text{H}^+]) - ([\text{H}^+]_0 - [\text{H}^+])\} = K_1[\text{H}^+](k_2 + k_3[\text{H}^+])([\text{H}^+]_0 - [\text{H}^+])[\text{H}_2\text{O}_2]_0 \quad (14)$$

3-2. The Neutral-to-Acidic Bifurcation. Let us first consider the bifurcation from neutral to acidic branches. In the neutral state, $[\text{H}^+] \approx 10^{-9} \sim 10^{-8} \text{ M} \ll [\text{H}^+]_0$. Equation 14 becomes

$$(k_2[\text{H}^+]_0 + k_0) \{K_1[\text{H}^+]([\text{SO}_3^{2-}]_0 - [\text{H}^+]_0) - [\text{H}^+]_0\} = K_1 k_2 [\text{H}^+]_0 [\text{H}_2\text{O}_2]_0 [\text{H}^+] \quad (15)$$

If $[\text{SO}_3^{2-}]_0$ is varied with fixed $[\text{H}_2\text{O}_2]_0$, $[\text{SO}_3^{2-}]_{0C}$ (the critical value of $[\text{SO}_3^{2-}]_0$ corresponding to the bifurcation point from the neutral to acidic stationary states) should correspond to the point where $\partial\text{pH}/\partial[\text{SO}_3^{2-}]_0$ approaches $\pm\infty$ in Figure 1, which, in turn, corresponds to $\partial[\text{H}^+]/\partial[\text{SO}_3^{2-}]_0 \rightarrow \pm\infty$. Therefore, one can determine the bifurcation point by differentiating eq 15 by $[\text{SO}_3^{2-}]_0$ with fixed $[\text{H}_2\text{O}_2]_0$ and $[\text{H}^+]_0$, and putting the coefficient of $\partial[\text{H}^+]/\partial[\text{SO}_3^{2-}]_0$ to be zero. This gives

$$([\text{H}_2\text{O}_2]_0 - [\text{SO}_3^{2-}]_{0C} + [\text{H}^+]_0) / [\text{H}^+]_0 = \{k_0 / (k_2[\text{H}^+]_0 + k_0)\} [\text{H}_2\text{O}_2]_0 / [\text{H}^+]_0 \quad (16)$$

The relation given by eq 16 is illustrated in Figure 3 along with the experimental results for 32.0 and 13.2 °C. Similar results have been obtained for 25.0 and 20.0 °C. Least-squares fitting of the experimental points to eq 16 gives k_2 for each temperature as summarized in Table 2.

3-3. The Acidic-to-Neutral Bifurcation. Now let us consider the acidic-to-neutral bifurcation point. Previous works^{2,3,6,16,17,19} suggest that k_3 and K_1 are of the order of $10^7 \text{ M}^{-2}\text{s}^{-1}$ and 10^7 M^{-1} , respectively. Equation 11 can then be approximated to

$$k_3[\text{H}^+]([\text{H}^+]_0 - [\text{H}^+]) ([\text{SO}_3^{2-}]_0 - [\text{H}_2\text{O}_2]_0 - [\text{H}^+]_0 + [\text{H}^+]) + k_0 ([\text{SO}_3^{2-}]_0 - [\text{H}^+]_0 + [\text{H}^+]) = 0 \quad (17)$$

To determine the bifurcation point, eq 17 is differentiated by $[\text{SO}_3^{2-}]_0$ with fixed $[\text{H}_2\text{O}_2]_0$ and $[\text{H}^+]_0$, and the coefficient of $\partial[\text{H}^+]/\partial[\text{SO}_3^{2-}]_0$ is put to 0, giving

$$[\text{H}^+]^2 - (2/3)([\text{H}_2\text{O}_2]_0 - [\text{SO}_3^{2-}]_0 + 2[\text{H}^+]_0)[\text{H}^+] + (1/3)\{[\text{H}^+]_0([\text{H}_2\text{O}_2]_0 - [\text{SO}_3^{2-}]_0 + [\text{H}^+]_0) - k_0/k_3\} = 0 \quad (18)$$

which determines the $[\text{H}^+]$ value at the bifurcation point to be

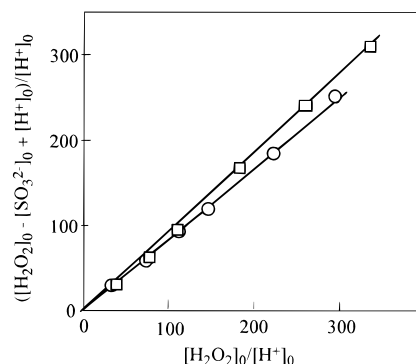


Figure 3. Plots of the experimental neutral-to-acidic bifurcation points against eq 16. Circles and squares represent the results at 32.0 °C and 13.2 °C, respectively. $[\text{H}^+]_0 = 1.15 \times 10^{-4} \text{ M}$ and $k_0 = 8.70 \times 10^{-3} \text{ s}^{-1}$.

TABLE 2: Rate Constants k_2 and k_3 and Equilibrium Constant K_1

temp/°C	$k_2/\text{M}^{-1}\text{s}^{-1}$	$k_3/10^6\text{M}^{-2}\text{s}^{-1}$	$k_3K_1^{-1}/\text{M}^{-1}\text{s}^{-1}$	$K_1/10^5\text{M}^{-1}$
13.2	8.7 ± 1.3	2.3 ± 0.1	38 ± 6	1.00 ± 0.16
20.0	11.7 ± 2.3	2.8 ± 0.3	39 ± 8	0.76 ± 0.15
25.0	13.8 ± 1.3	3.0 ± 0.3	30 ± 1	0.91 ± 0.04
32.0	16.4 ± 1.7	3.9 ± 0.3	22 ± 4	1.04 ± 0.18

$$[\text{H}^+]_C = (1/3)([\text{H}_2\text{O}_2]_0 - [\text{SO}_3^{2-}]_0 + 2[\text{H}^+]_0) \pm (1/3)R \quad (19)$$

where

$$R \equiv [([\text{H}_2\text{O}_2]_0 - [\text{SO}_3^{2-}]_0 + 2[\text{H}^+]_0)^2 - 3\{[\text{H}^+]_0([\text{H}_2\text{O}_2]_0 - [\text{SO}_3^{2-}]_0 + 2[\text{H}^+]_0) - [\text{H}^+]_0^2 - k_0/k_3\}]^{1/2} \quad (20)$$

Inserting eq 19 into eq 17, one gets

$$2X^3 + 3X^2 - 3X - 2 + 9h(3P - 2X - 1) \pm 2\{X^2 + X + 1 + 3h\}R = 0 \quad (21)$$

where

$$X \equiv ([\text{H}_2\text{O}_2]_0 - [\text{SO}_3^{2-}]_{0C}) / [\text{H}^+]_0 \quad (22)$$

$$P \equiv [\text{H}_2\text{O}_2]_0 / [\text{H}^+]_0 \quad (23)$$

and

$$h \equiv k_0/k_3[\text{H}^+]_0^2 \quad (24)$$

R can now be written as

$$R = (X^2 + X + 1 + 3h)^{1/2} \quad (25)$$

Since $h \sim 0.1$ and $X \gg 1$, except for one or two experimental points with lower $[\text{H}_2\text{O}_2]_0$ values, R is approximated to

$$R = X\{1 + X^{-1} + (1 + 3h)X^{-2}\}^{1/2} \approx X\{1 + (1/2)X^{-1} + (3/8)X^{-2} - (1/4)X^{-3} - (1/8)X^{-4} + (3/4)hX^{-2}\{2 - X^{-1} - X^{-2}\} - (9/8)h^2X^{-4}\} \quad (26)$$

taking up to the second order in the Taylor expansion. Using eq 26 in eq 21,

$$X + (13/27) - (1/9)X^{-2} - (1/27)X^{-3} - (2/3)h\{6P - 6X - 3 - (1/2)X^{-1} + X^{-2} + (1/2)X^{-3}\} + h^2\{X^{-1} - X^{-2} - X^{-3}\} - h^3X^{-3} \approx 0 \quad (27)$$

Under the assumption of $X \gg 1$ and $h \approx 0.1$, eq 27 can further be approximated to

$$X + (13/27) - 2h(2P - 2X - 1) \approx 0$$

or

$$X \approx 4hP/(1 + 4h) - (2h + 13/27)/(1 + 4h) \quad (28)$$

The fitting of eq 28 to the experimental points is illustrated in Figure 4 for 32.0 and 13.2 °C. In these cases, the points corresponding to the lowest values of $[H_2O_2]_0$ do not fit the line since $X \gg 1$ does not hold. Similar results are obtained for 25 and 20 °C. From the slope, $4h/(1 + 4h)$, we can determine k_3 as shown in Table 2.

3-4. Estimation of K_1 : A Higher Order Approximation in the Neutral-to-Acidic Bifurcation. In the above-mentioned analysis of the neutral-to-acidic bifurcation in section 3-2, we have neglected terms $[H^+]$ and $k_3[H^+]$ in eq 14 to obtain eq 15. Here we shall try to retain the $k_3[H^+]$ term in eq 14 for the purpose of estimating K_1 . Now eq 14 becomes

$$\{(k_2 + k_3[H^+])[H^+]_0 + k_0\}\{K_1[H^+](SO_3^{2-}]_0 - [H^+]_0) - [H^+]_0\} = K_1[H^+](k_2 + k_3[H^+])[H^+]_0[H_2O_2]_0 \quad (29)$$

Differentiating eq 29 by $[SO_3^{2-}]_0$ with fixed $[H_2O_2]_0$ and $[H^+]_0$ and putting the coefficient of $\partial[H^+]/\partial[SO_3^{2-}]_0$ to be 0, one gets

$$[H^+]_C = (k_0/2k_3)([SO_3^{2-}]_0 - [H^+]_0)/[H^+]_0([H_2O_2]_0 - [SO_3^{2-}]_0 + [H^+]_0) - (1/2K_1)[H^+]_0/([H_2O_2]_0 - [SO_3^{2-}]_0 + [H^+]_0) - k_2/2k_3 \quad (30)$$

Inserting eq 30 into eq 29, one gets, after some manipulations,

$$([H_2O_2]_0 - [SO_3^{2-}]_{0C} + [H^+]_0)/[H^+]_0 - \{k_0/(k_0 + k_2[H^+]_0)\}([H_2O_2]_0/[H^+]_0) = (k_3/K_1)[H^+]_0/(k_0 + k_2[H^+]_0) \pm 2(k_0k_3/K_1)^{1/2}[H_2O_2]_0^{1/2}/(k_0 + k_2[H^+]_0) \quad (31)$$

If one defines

$$X \equiv ([H_2O_2]_0 - [SO_3^{2-}]_{0C} + [H^+]_0)/[H^+]_0 - \{k_0/(k_0 + k_2[H^+]_0)\}([H_2O_2]_0/[H^+]_0) \quad (32)$$

and

$$\alpha \equiv \pm 2\{(k_0k_3/K_1)[H^+]_0\}^{1/2}/(k_0 + k_2[H^+]_0) \quad (33)$$

then eq 31 can be written as

$$X = \beta + \alpha([H_2O_2]_0/[H^+]_0)^{1/2} \quad (34)$$

where

$$\beta \equiv (k_3/K_1)[H^+]_0/(k_0 + k_2[H^+]_0)$$

Note that the estimation of k_2 in section 3-2 is based on the approximation $X = 0$.

Plots of X against $([H_2O_2]_0/[H^+]_0)^{1/2}$ are illustrated in Figure 5 for 13.2 and 32.0 °C. Similar plots can be obtained for 20.0 and 25.0 °C. Least-squares fitting of the experimental points to eq 34 gives α for each temperature, from which k_3/K_1 is determined through eq 33 using the k_2 values determined above (Table 2). Combined these with k_3 determined above, K_1 can be estimated as summarized in Table 2.

3-5. Temperature Dependence. Arrhenius plots for k_2 and k_3 obtained above are given in Figures 6 and 7, respectively,

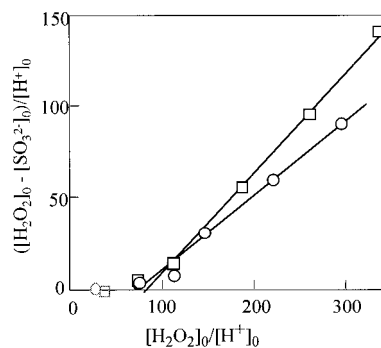


Figure 4. Plots of the experimental acidic-to-neutral bifurcation points against eq 28. Circles and squares represent the results at 32.0 °C and 13.2 °C, respectively. $[H^+]_0 = 1.15 \times 10^{-4}$ M and $k_0 = 8.70 \times 10^{-3}$ s $^{-1}$.

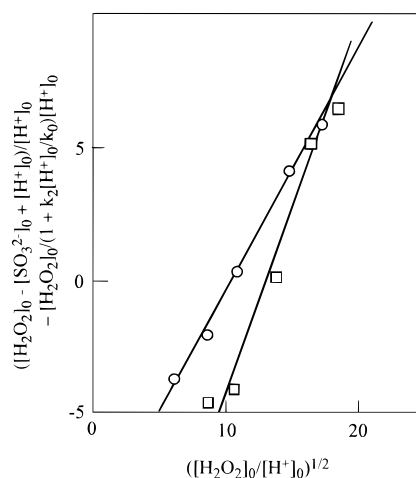


Figure 5. Plots of the experimental neutral-to-acidic bifurcation points against eq 34. Circles and squares represent the results at 32.0 °C and 13.2 °C, respectively. $[H^+]_0 = 1.15 \times 10^{-4}$ M and $k_0 = 8.70 \times 10^{-3}$ s $^{-1}$.

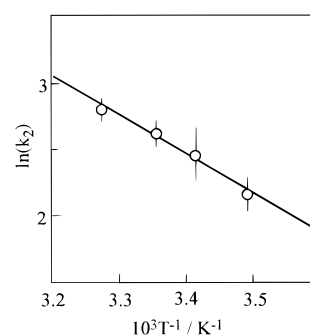


Figure 6. Arrhenius plot of k_2 .

from which the temperature dependence is determined as

$$k_2 \text{ (M}^{-1}\text{s}^{-1}\text{)} = (1.19 \times 10^6)\exp(-\Delta H_2^\ddagger/RT) \quad (35)$$

where

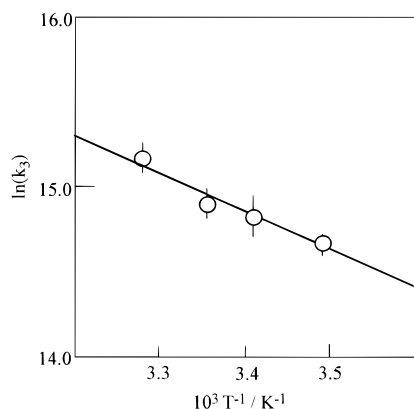
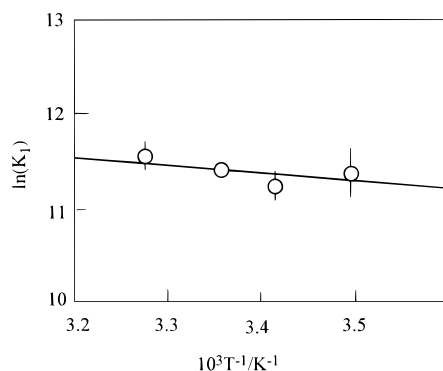
$$\Delta H_2^\ddagger = 28.2 \pm 1.2 \text{ kJ}\cdot\text{M}^{-1} \quad (36)$$

and

$$k_3 \text{ (M}^{-2}\text{s}^{-1}\text{)} = (5.93 \times 10^9)\exp(-\Delta H_3^\ddagger/RT) \quad (37)$$

where

$$\Delta H_3^\ddagger = 18.7 \pm 1.7 \text{ kJ}\cdot\text{M}^{-1} \quad (38)$$

Figure 7. Arrhenius plot of k_3 .Figure 8. Temperature dependence of K_1 .

Temperature dependence of K_1 is illustrated in Figure 8, from which one obtains

$$K_1 (\text{M}^{-1}) = (1.8 \times 10^6) \exp(-\Delta H_1/RT) \quad (39)$$

where

$$\Delta H_1 = 7.4 \pm 4.3 \text{ kJ} \cdot \text{M}^{-1} \quad (40)$$

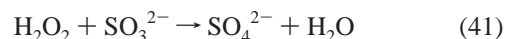
4. Discussion

The only available literature value for k_2 ($\approx 7 \text{ M}^{-1}\text{s}^{-1}$) has been determined by the stopped-flow measurement.²⁰ The present result is the first which gives reliable values under the flow condition with temperature dependence. The relatively smaller values of $k_2 = 8\text{--}16 \text{ M}^{-1}\text{s}^{-1}$ obtained here for $13.2\text{--}32.0 \text{ }^\circ\text{C}$, compared with k_3 , are essential for the clear appearance of the bistability.

On the other hand, the rate constant for the autocatalytic process (eq 3) has been estimated to be $k_3 \approx 6 \times 10^6$ and $1.5 \times 10^7 \text{ M}^{-2}\text{s}^{-1}$ for 12 and $25 \text{ }^\circ\text{C}$, respectively, in the literature.^{2,6,16,17,19} The present systematic measurement gives $k_3 = (2.3\text{--}3.9) \times 10^6 \text{ M}^{-2}\text{s}^{-1}$ for $13.2\text{--}32.0 \text{ }^\circ\text{C}$, which are a little bit smaller than the previous estimations. Nevertheless, the k_3 value is still large enough for the autocatalytic process to proceed effectively. The equilibrium constant K_1 is found to be of the order of 10^5 M^{-1} , which is smaller than the value of ca. 10^7 M^{-1} suggested previously.² Nevertheless, it is sufficiently large to guarantee that reaction 1 functions as the switching process, where either $[\text{H}^+] \approx 0$ for $[\text{SO}_3^{2-}] > 0$ or $[\text{SO}_3^{2-}] \approx 0$ for $[\text{H}^+] > 0$ holds.

The experimental results and analysis presented here provide reliable values of rate constants k_2 and k_3 and equilibrium constant K_1 with reasonable accuracy, together with their temperature dependencies. The relatively small activation energy of $\Delta H_3^\ddagger = 18.7 \text{ kJ} \cdot \text{M}^{-1}$ for the autocatalytic process results in the insensitivity of the rate to the temperature change. This encourages us to try to construct a temperature-insensitive chemical oscillator system that would simulate living systems¹⁸ by combining this subsystem with an appropriate negative-feedback channel to cancel out the temperature dependence further.

Finally, in addition to the main reaction scheme eqs 1–3 employed here, the reaction



is also known to occur in this system. McArdle and Hoffmann¹⁷ have given $k_{41} \approx 0.2 \text{ M}^{-1}\text{s}^{-1}$ at $15 \text{ }^\circ\text{C}$ by stopped flow measurements. Although k_{41} is an order of magnitude smaller than k_2 , eq 41 would generally contribute to the results when $[\text{SO}_3^{2-}]$ is large, since $V_2 \approx k_2[\text{H}_2\text{O}_2][\text{HSO}_3^-]$ where $[\text{HSO}_3^-] \approx [\text{H}^+]_0 = \text{constant}$. However, contribution of eq 41 can be ignored in the present analysis where only the bifurcation point is measured under the CSTR condition. The situation may simply be explained as follows: when the system approaches the bifurcation point from the neutral side, $[\text{SO}_3^{2-}]$, the concentration of free sulfite ions, approaches 0, resulting in an infinitely small rate of eq 41, whereas V_2 keeps the value, $V_2 \approx k_2[\text{H}_2\text{O}_2][\text{H}^+]_0$. Hence, under the stationary flow condition, only negligibly small contribution arises from eq 41 in the determination of the bifurcation value, $[\text{SO}_3^{2-}]_{\text{OC}}$, which is determined solely by the balance of V_2 and the flow-in and flow-out of species. In the case of the acidic-to-neutral bifurcation, the concentration of the free sulfite ion is kept as $[\text{SO}_3^{2-}] \approx 0$ in the acidic stationary state so that no contribution from eq 41 is expected to the bifurcation point.

Acknowledgment. One of the authors (I.H.) acknowledges helpful discussions with Professor Gyula Rábai, Debrecen, Hungary. He also acknowledges Dr. N. Okazaki's help at the beginning stage of the experiments.

References and Notes

- (1) Kaminaga, A.; Rábai, G.; Hanazaki, I. *Chem. Phys. Lett.* **1998**, *284*, 109.
- (2) Rábai, G.; Kustin, K.; Epstein, I. R. *J. Am. Chem. Soc.* **1989**, *111*, 3870.
- (3) Rábai, G.; Kustin, K.; Epstein, I. R. *J. Am. Chem. Soc.* **1989**, *111*, 8271.
- (4) Mori, Y.; Hanazaki, I. *J. Phys. Chem.* **1992**, *96*, 9083.
- (5) Mori, Y.; Hanazaki, I. *J. Phys. Chem.* **1993**, *97*, 7375.
- (6) Rábai, G.; Hanazaki, I. *J. Phys. Chem.* **1996**, *100*, 15454.
- (7) Frerichs, G. A.; Thompson, R. C. *J. Phys. Chem.* **1998**, *102*, 8142.
- (8) Rábai, G.; Kaminaga, A.; Hanazaki, I. *Chem. Commun.* **1996**, 2181.
- (9) Rábai, G.; Hanazaki, I. *J. Am. Chem. Soc.* **1997**, *119*, 1458.
- (10) Edblom, E. C.; Luo, Y.; Orban, M.; Kustin, K.; Epstein, I. R. *J. Phys. Chem.* **1989**, *93*, 2722.
- (11) Hanazaki, I.; Rábai, G. *J. Chem. Phys.* **1996**, *105*, 9912.
- (12) Rábai, G.; Epstein, I. R. *Inorg. Chem.* **1989**, *28*, 732.
- (13) Rábai, G.; Kaminaga, A.; Hanazaki, I. *J. Chem. Phys.* **1996**, *100*, 16441.
- (14) Rábai, G.; Hanazaki, I. *J. Phys. Chem.* **1996**, *100*, 10615.
- (15) Okazaki, N.; Rábai, G.; Hanazaki, I. *J. Phys. Chem. A* **1999**, *103*, 10915.
- (16) Drexler, C.; Elias, H.; Fecher, B.; Wannowius, K. *J. Ber. Bunsen-Ges. Phys. Chem.* **1992**, *96*, 481.
- (17) McArdle, J. V.; Hoffmann, M. R. *J. Phys. Chem.* **1983**, *87*, 5425.
- (18) Rábai, G.; Hanazaki, I. *Chem. Commun.* **1999**, 1965.
- (19) Jaeschke, W. A.; Herrmann, G. *J. ACS Symp. Series* **1987**, *349*, 142.